



## Calculated Phase Diagram for the Transition in Ce

Johansson, Børje; Abrikosov, I. A.; Aldén, Magnus; Ruban, Andrei; Skriver, Hans Lomholt

*Published in:*  
Physical Review Letters

*Link to article, DOI:*  
[10.1103/PhysRevLett.74.2335](https://doi.org/10.1103/PhysRevLett.74.2335)

*Publication date:*  
1995

*Document Version*  
Publisher's PDF, also known as Version of record

[Link back to DTU Orbit](#)

*Citation (APA):*  
Johansson, B., Abrikosov, I. A., Aldén, M., Ruban, A., & Skriver, H. L. (1995). Calculated Phase Diagram for the Transition in Ce. *Physical Review Letters*, 74(12). <https://doi.org/10.1103/PhysRevLett.74.2335>

---

### General rights

Copyright and moral rights for the publications made accessible in the public portal are retained by the authors and/or other copyright owners and it is a condition of accessing publications that users recognise and abide by the legal requirements associated with these rights.

- Users may download and print one copy of any publication from the public portal for the purpose of private study or research.
- You may not further distribute the material or use it for any profit-making activity or commercial gain
- You may freely distribute the URL identifying the publication in the public portal

If you believe that this document breaches copyright please contact us providing details, and we will remove access to the work immediately and investigate your claim.

## Calculated Phase Diagram for the $\gamma \rightleftharpoons \alpha$ Transition in Ce

B. Johansson, I. A. Abrikosov, and M. Aldén

*Condensed Matter Theory Group, Physics Department, Uppsala University, S-75121 Uppsala, Sweden*

A. V. Ruban and H. L. Skriver

*Center for Atomic-scale Materials Physics and Physics Department, Technical University of Denmark, DK-2800 Lyngby, Denmark*

(Received 28 October 1994)

We have calculated the pressure-temperature phase diagram of the  $\gamma \rightleftharpoons \alpha$  isostructural transition in Ce on the basis of the Mott transition model. The theory correctly describes the linear variation of the transition temperature with pressure and the existence of a critical point. The quantitative agreement with the experimental diagram is good. The influence of different free energy contributions (configurational, magnetic, and vibrational) on the phase transition in Ce is discussed.

PACS numbers: 71.45.Nt, 64.70.Kb, 71.28.+d

Cerium is one of the most fascinating elements in the periodic table. It has, in particular, an extremely rich phase diagram with at least five allotropic forms [1]. Most attention has been focused on the  $\gamma \rightleftharpoons \alpha$  isostructural phase transition where the high-volume face-centered cubic (fcc)  $\gamma$  phase collapses into the low-volume fcc  $\alpha$  phase at a pressure of about 7 kbar. There is little doubt about the electronic nature of this transition, and a great number of theoretical investigations have dealt with the electronic properties of cerium [2–15].

The unusual behavior of Ce has been described within a number of models that may be classified into three groups. The first is the promotional model of Zachariasen and Pauling [2] which explains the transition as a promotion of the Ce 4*f* electron into the 5*d*-6*s* valence band by the movement of a sharp *f* level from below to above the Fermi level [3]. However, neither experimental studies [1] nor calculations [4–7] were able to confirm this idea.

The second model is the so-called Kondo volume-collapse (KVC) model [8–12], where one assumes that the transition is caused by a change in the conduction electron screening of the Ce 4*f* electron, which is considered to be localized in both the  $\gamma$  and the  $\alpha$  phase. In this model the Anderson impurity Hamiltonian is used to describe spectroscopic [10,11] as well as thermodynamic [8,12] properties. In particular, Allen and Martin [8] and later Allen and Liu [12] calculated a pressure-temperature (*P*-*T*) phase diagram for the  $\gamma \rightleftharpoons \alpha$  transition and obtained good agreement between the theoretical and experimental values for the critical point. This fact has been viewed as strong support for the KVC model. However, on the basis of the analysis of experimental data, Koskenmaki and Gschneidner [1] emphasized the fact that the transition temperature depends linearly on pressure, and this is in contrast to the significant curvature found in the theoretical diagram of Ref. [12].

The third model is the Mott transition model advocated by Johansson [4]. According to this, the nature of the 4*f* states in Ce changes from local nonbonding in the  $\gamma$

phase to itinerant bonding in the  $\alpha$  phase. A number of recent *ab initio* calculations, where one assumes that the 4*f* electron is localized in  $\gamma$ -Ce but delocalized in  $\alpha$ - and  $\alpha'$ -Ce, have given excellent results for the ground state properties of  $\gamma$ - and  $\alpha$ -Ce [7,13–15] as well as for the  $\alpha \rightleftharpoons \alpha'$  transition [16]. Moreover, by applying the self-interaction corrected (SIC) local density approximation (LDA) Szotek, Temmerman, and Winter [14] and Svane [15] find that in spite of the dramatic change in the electronic structure at the transition, the difference in total energy between  $\gamma$ - and  $\alpha$ -Ce is of the order of mRy. A similar energy difference is found in Ref. [13], and this is exactly what is required to describe the transition in the Mott transition model.

Until now the only quantitative description of Ce at finite temperatures within the Mott transition picture is provided by the semiempirical band model of Rainford and Edwards [17]. In the present Letter we therefore calculate the *P*-*T* diagram for the  $\gamma \rightleftharpoons \alpha$  transition in Ce based on the Mott picture and the thermodynamic model illustrated in Fig. 1. According to this, there are at zero temperature two phases in Ce, a low-volume  $\alpha$  phase which is stable, and a high-volume  $\gamma$  phase which is metastable. The resulting binding energy curve viewed as a function of volume is formed by two branches corresponding to  $\alpha$ - and  $\gamma$ -Ce, respectively, which cross at some intermediate volume. The transition between  $\alpha$ - and  $\gamma$ -Ce represented by the common tangent in Fig. 1(a) occurs when the lattice is expanded, and from the experimental data of Ref. [1] the transition pressure is deduced to be  $-6$  kbar.

As the temperature increases the state ( $\alpha$  or  $\gamma$ ) which is metastable may be thermally populated. Hence, there is a probability *x* of finding a  $\gamma$ -Ce atom in the system and a  $1 - x$  probability of finding an  $\alpha$ -Ce atom. Therefore, we may consider our system as a pseudoalloy  $\text{Ce}^{\gamma}_x\text{Ce}^{\alpha}_{1-x}$  and write its free energy  $F_{\text{alloy}}$  for any "concentration" *x*, volume *V*, and temperature *T* as

$$F_{\text{alloy}}(x, V, T) = E(x, V) - TS(x) + F_{\text{IV}}(x, V, T). \quad (1)$$

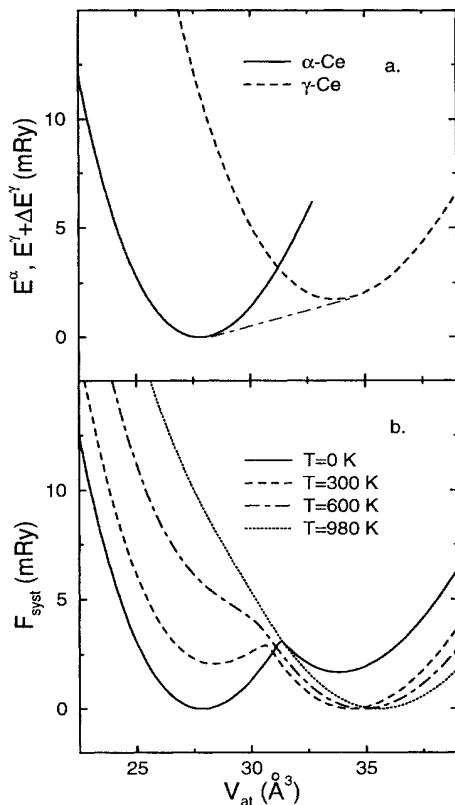


FIG. 1. Binding energy curves for  $\alpha$ - and  $\gamma$ -Ce (a) and the free energy of the system  $F_{\text{sys}}$  at different temperatures (b) as a function of atomic volume  $V_{\text{at}}$ . The energies in (a) are relative to the minimum energy for  $\alpha$ -Ce, while in (b) they are relative to the minimum value of  $F_{\text{sys}}$  at the corresponding temperature. The dot-dashed line in (a) corresponds to the experimental value of  $-6$  kbar for the transition pressure at zero temperature. The energy shift  $\Delta E^\gamma$  in Eq. (5) has been adjusted to reproduce this transition pressure.

Here,  $E$  is an average internal energy per atom in the pseudoalloy at  $T = 0$ ,  $S$  the entropy, and  $F_{1v}$  the free energy of the lattice vibrations.

In the model, we include the configurational mixing entropy, which in the mean-field (MF) approximation may be written as

$$S_{\text{conf}}(x) = -k_B[x \ln x + (1-x) \ln(1-x)], \quad (2)$$

where  $k_B$  is the Boltzmann constant, and the magnetic entropy from the localized magnetic moment on the  $\gamma$ -Ce atoms. Assuming that for temperatures of interest only the ground state multiplet with total angular momentum  $J = 5/2$  is appreciably populated, the latter may be calculated from

$$S_{\text{magn}}(x) = k_B x \ln(2J + 1). \quad (3)$$

Finally, the vibrational free energy  $F_{1v}(x, V, T)$  is estimated in the Debye-Grüneisen model [18] from the ground state binding energy curve for any particular  $x$ .

Since we are dealing with a pseudoalloy, the alloy concentration is not a free parameter, and only those concentrations  $x_{\text{eq}}$  will occur which for a fixed volume and temperature minimize the free energy (1) in the concentration interval  $0 \leq x \leq 1$ . Hence, we arrive at the final expression for the free energy of the system

$$F_{\text{sys}}(V, T) = F_{\text{alloy}}(x_{\text{eq}}(V, T), V, T). \quad (4)$$

It follows that if we calculate the system free energy as a function of volume we may obtain Gibbs free energy  $G = F + pV$ , where  $p$  is the pressure, and determine the transition pressure of the  $\gamma \rightleftharpoons \alpha$  transition at any temperature. Hence, we may calculate the  $P$ - $T$  phase diagram for Ce within the Mott transition model.

To realize such a program we need a good description of the initial  $\alpha$  and  $\gamma$  states as well as of the alloy total energy  $E(x, V)$ . In particular, it is important for the accuracy of the calculated phase diagram that the equilibrium volumes of pure  $\gamma$ - and  $\alpha$ -Ce are well reproduced by the total energy calculations. For this purpose we use the scalar-relativistic linear muffin-tin orbitals (LMTO) method within the atomic sphere approximation (ASA) and in the tight-binding representation [19–21] in conjunction with a Green's function technique and treat the alloy within a scheme based on the single-site coherent-potential approximation (SS-CPA) [22,23]. In all the calculations the  $5s$  and  $5p$  states are treated as semicores, while the remaining core states are frozen.

To describe paramagnetic  $\alpha$ -Ce we regard the  $4f$  electron as a delocalized valence electron. Note that such an assumption together with LDA leads to an underestimate of the equilibrium volume and an overestimate of the bulk modulus compared with the experimental values (Table I). However, this is basically an effect of using the LDA rather than an effect associated with any special properties of  $\alpha$ -Ce, because for the two closely related elements, La and Th, we find similar deviations between the LDA results and the experimental data, as may also be seen in Table I. Moreover, Söderlind *et al.* [26] found that the ground state parameters of  $\alpha$ -Ce are very sensitive to the approximation used for the exchange-correlation functional. When we apply the Becke-Perdew gradient correction (GGA, Ref. [27]) to the exchange-correlation potential we obtain a much better agreement between the calculated and experimental atomic volume and bulk modulus for  $\alpha$ -Ce as well as for La and Th (Table I). For this reason, we chose to describe pure  $\alpha$ -Ce and the  $\alpha$ -Ce atoms in the alloy within this approximation for exchange and correlation.

One may account for the localized  $4f$  electron in  $\gamma$ -Ce by means of the SIC-LDA scheme [14,15]. However, in an alloy this becomes numerically very complicated, and we therefore chose the approach used earlier in Ref. [7]; i.e., we consider one  $4f$  electron in  $\gamma$ -Ce as fully localized by treating it as part of the inert core, but leave  $f$  functions

TABLE I. Calculated and experimental ground state atomic volume  $V$  (in  $\text{\AA}^3$ ) and bulk modulus  $B$  (in kbar) for the pure  $\alpha$ -Ce,  $\gamma$ -Ce, fcc La, and fcc Th.

Method	$\alpha$ -Ce		$\gamma$ -Ce		La		Th	
	$V$	$B$	$V$	$B$	$V$	$B$	$V$	$B$
LDA <sup>a</sup>	24.45	477	33.70	312	33.18	320	30.05	618
GGA <sup>a</sup>	27.74	391	37.31	288	37.07	268	32.63	572
SIC-LDA <sup>b</sup>	25.90	443	34.00	340				
SIC-LDA <sup>c</sup>	24.80	484	32.44	310				
Expt.	28.17 <sup>d</sup>	270 <sup>e</sup>	34.36 <sup>d</sup>	239 <sup>f</sup>	37.31 <sup>d</sup>	243 <sup>f</sup>	32.87 <sup>d</sup>	543 <sup>f</sup>

<sup>a</sup>This work.

<sup>b</sup>Reference [14].

<sup>c</sup>Reference [15].

<sup>d</sup>Reference [24].

<sup>e</sup>Taken from Ref. [13].

<sup>f</sup>Reference [25], value for La is given for hexagonal structure.

in the LMTO valence basis set. Using the Vosko-Wilk-Nusair parametrization [28] of the exchange-correlation energy density and potential our paramagnetic calculations for the equilibrium atomic volume and bulk modulus of  $\gamma$ -Ce (Table I) show excellent agreement with the results obtained from the SIC-LDA calculations [14,15] as well as with experimental values. We therefore use this set of approximations for pure  $\gamma$ -Ce and for  $\gamma$ -Ce atoms in the alloy.

Within the frozen core approximation [20], used in our simplified description of  $\gamma$ -Ce, the contribution to the energy from the localized  $4f$  electron is discarded. We must therefore align the energies of the two phases of Ce by an energy shift  $\Delta E^\gamma$  added, for instance, to the total energy of  $\gamma$ -Ce [29]. We emphasize that this is the only adjustable parameter in our model and that it is introduced for technical reasons rather than as a matter of principles. The internal energy  $E(x, V)$  in (1) may now be written in the form

$$E(x, V) = (1 - x)E^\alpha(x, V) + x[E^\gamma(x, V) + \Delta E^\gamma], \quad (5)$$

where  $E^j(x, V)$ ,  $j = \alpha, \gamma$  is the first-principle total energy calculated per  $\alpha$  (or  $\gamma$ ) atom as allowed by the ASA within the SS-CPA [22].

The calculated phase diagram for the  $\gamma \rightleftharpoons \alpha$  transition in Ce is shown in Fig. 2 together with the experimental phase diagram taken from Ref. [1]. It is seen that the present theory, labeled MF in the figure, correctly describes the salient features of the phase diagram, i.e., the linear dependence of the transition temperature on pressure and the existence of a critical point. The zero pressure transition temperature is calculated to be 135 K, in excellent agreement with the experimental value  $141 \pm 10$  K. The critical point is found at 980 K and 38.6 kbar, in fair agreement with experiment ( $600 \pm 50$  K,  $19.6 \pm 2$  kbar, Ref. [1]). A small overestimate of the critical temperature and pressure is to be expected because of the application of the mean-field approximation for the

entropy. If we use the more elaborate cluster variation method (CVM) in conjunction with the CPA Connolly-Williams scheme for calculating interatomic interactions [23], we obtain an even better result for the calculated  $P$ - $T$  diagram (see Fig. 2).

Within the framework of our model we now analyze the influence on the calculated phase diagram of the different contributions to the free energy (1). First, we find that the vibrational contribution has little effect on the phase diagram (Fig. 2). This is to be expected, because the ground state parameters for  $\alpha$ - and  $\gamma$ -Ce are close to each other (Table I), which means that the free energy

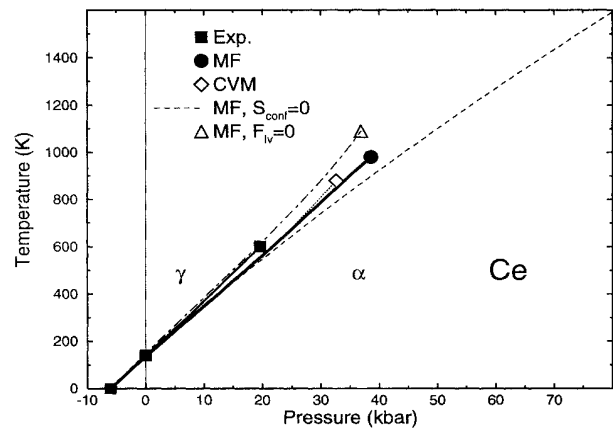


FIG. 2. Pseudoequilibrium pressure-temperature phase diagram for Ce. The experimental result is taken for [1] and shown by the full line and filled squares. The zero temperature value is obtained by extrapolation. The diagram calculated within the MF approximation and with all the contributions to the free energy included is shown by the heavy full line. The corresponding critical point is shown by the full circle. The results obtained by the CVM are indicated by the dotted line and the open diamond. The dashed line corresponds to a MF phase diagram where the effect of alloying is neglected, i.e.,  $S_{\text{conf}} \equiv 0$ , and the dot-dashed line with the open triangle corresponds to the MF diagram calculated without the vibrational contribution to the free energy, i.e.,  $F_{\text{vib}} \equiv 0$ .

of the lattice vibrations in the two phases as estimated in the Debye-Grüneisen model [18] will not differ much. Second, our calculations show that close to the ground state volumes of pure  $\alpha$ - and  $\gamma$ -Ce, between which the transition takes place, the equilibrium concentrations  $x_{\text{eq}}$  are very close to 0 or 1, respectively, up to temperatures of about 500 K. This means that at low temperatures we may neglect the alloying effects when calculating the transition pressure. If we also neglect the vibrational free energy, the only entropic contribution left is that of the magnetic moment on the Ce atoms, which is zero in the  $\alpha$  phase and  $k_B \ln(2J + 1)$  in the  $\gamma$  phase. Thus, this term is responsible for the low temperature part of the phase diagram and, in particular, for the stabilization of  $\gamma$ -Ce at temperatures above 135 K. Moreover, the transition pressure may now easily be estimated as [30]

$$P(T) = P_0 + T \frac{k_B \ln(2J + 1)}{V_0^\gamma - V_0^\alpha}, \quad (6)$$

where the subscript 0 refers to  $T = 0$ , and this immediately explains the observed linear dependence of the transition temperature on the pressure. Finally, for the artificial, intermediate volumes the equilibrium concentration  $x_{\text{eq}}$  is substantial already at relatively low temperatures (about 300 K). This results in a softening of the crossover between the two branches of the free energy, as shown in Fig. 1(b), and in the end to the occurrence of the critical point. The last statement is illustrated in Fig. 2. When the effect of alloying is completely neglected, the low temperature behavior of the phase diagram is almost identical to that of the complete calculation, but the critical point is lost.

In summary, we have calculated the  $P$ - $T$  phase diagram of the  $\gamma \rightleftharpoons \alpha$  transformation in Ce based on the Mott transition picture. The theory correctly describes the topology of the experimentally observed phase diagram, i.e., the linear variation of the transition temperature with pressure and the existence of a critical point.

The Center for Atomic-scale Materials Physics is sponsored by the Danish National Research Foundation. The work of I. A. A. and A. V. R. was in part supported by the Swedish Material Consortium No. 9 and Grant No. MQQ000 from the International Science Foundation, respectively. I. A. A. also would like to acknowledge valuable discussions with Professor I. S. Sandalov.

- 
- [1] D. G. Koskenmaki and K. A. Gschneidner, Jr., in *Handbook on the Physics and Chemistry of Rare Earths*, edited by K. A. Gschneidner, Jr. and L. Eyring (North-Holland, Amsterdam, 1979), Vol. I, p. 337.  
 [2] W. H. Zachariasen, as quoted by A. W. Lawson and T. Y. Tang, *Phys. Rev.* **76**, 301 (1949); L. Pauling, as quoted by A. F. Schuch and J. H. Sturdivant, *J. Chem. Phys.* **18**, 145 (1950).

- [3] B. Coqblin and A. Blandin, *Adv. Phys.* **17**, 281 (1968); R. Ramirez and L. M. Falicov, *Phys. Rev. B* **3**, 2425 (1971); L. L. Hirst, *J. Phys. Chem. Solids* **35**, 1285 (1974).  
 [4] B. Johansson, *Philos. Mag.* **30**, 469 (1974).  
 [5] D. Glötzel, *J. Phys. F* **8**, L163 (1978); R. Podloucky and D. Glötzel, *Phys. Rev. B* **27**, 3390 (1983).  
 [6] W. E. Pickett, A. J. Freeman, and D. D. Koelling, *Phys. Rev. B* **23**, 1266 (1981).  
 [7] B. I. Min, H. J. F. Jansen, T. Oguchi, and A. J. Freeman, *Phys. Rev. B* **34**, 369 (1986).  
 [8] J. W. Allen and R. M. Martin, *Phys. Rev. Lett.* **49**, 1106 (1982).  
 [9] M. Lavagna, C. Lacroix, and M. Cyrot, *Phys. Lett.* **90A**, 210 (1982); *J. Phys. F* **13**, 1007 (1983).  
 [10] O. Gunnarsson and K. Schönhammer, *Phys. Rev. B* **28**, 4315 (1983).  
 [11] L. Z. Liu, J. W. Allen, O. Gunnarsson, N. E. Cristensen, and O. K. Andersen, *Phys. Rev. B* **45**, 8934 (1992).  
 [12] J. W. Allen and L. Z. Liu, *Phys. Rev. B* **46**, 5047 (1992).  
 [13] O. Eriksson, M. S. S. Brooks, and B. Johansson, *Phys. Rev. B* **41**, 7311 (1990).  
 [14] Z. Szotek, W. M. Temmerman, and H. Winter, *Phys. Rev. Lett.* **72**, 1244 (1994).  
 [15] A. Svane, *Phys. Rev. Lett.* **72**, 1248 (1994).  
 [16] J. M. Wills, O. Eriksson, and A. M. Boring, *Phys. Rev. Lett.* **67**, 2215 (1991); O. Eriksson, J. M. Wills, and A. M. Boring, *Phys. Rev. B* **46**, 12981 (1992).  
 [17] B. D. Rainford and D. M. Edwards, *J. Magn. Magn. Mater.* **63&64**, 557 (1987).  
 [18] V. L. Moruzzi, J. F. Janak, and K. Schwarz, *Phys. Rev. B* **37**, 790 (1988).  
 [19] O. K. Andersen, O. Jepsen, and D. Glötzel, in *Highlights of Condensed-Matter Theory*, edited by F. Bassani, F. Fumi, and M. P. Tosi (North-Holland, New York, 1985).  
 [20] O. Gunnarsson, O. Jepsen, and O. K. Andersen, *Phys. Rev. B* **27**, 7144 (1983).  
 [21] H. L. Skriver, *The LMTO Method* (Springer-Verlag, Berlin, 1984).  
 [22] D. D. Johnson, D. M. Nicholson, F. J. Pinski, B. L. Gyorffy, and G. M. Stocks, *Phys. Rev. B* **41**, 9701 (1990).  
 [23] I. A. Abrikosov, A. V. Ruban, D. Ya. Kats, and Yu. H. Vekilov, *J. Phys. Condens. Matter* **5**, 1271 (1993).  
 [24] J. Donohue, *The Structure of the Elements* (John Wiley & Sons, Inc., New York, 1974).  
 [25] C. Kittel, *Introduction to Solid State Physics* (John Wiley & Sons, Inc., New York, 1986).  
 [26] P. Söderlind, O. Eriksson, B. Johansson, and J. M. Wills, *Phys. Rev. B* **50**, 7291 (1994).  
 [27] J. P. Perdew, *Phys. Rev. B* **33**, 8822 (1986); A. D. Becke, *Phys. Rev. A* **38**, 3098 (1988).  
 [28] S. H. Vosko, L. Wilk, and M. Nusair, *Can. J. Phys.* **58**, 1200 (1980).  
 [29] We find that a  $\Delta E^\gamma$  of  $-12.5199$  Ry leads to the experimental value of  $-6$  kbar for the transition pressure at zero temperature and an energy difference between the  $\gamma$  and  $\alpha$  phases of 1.75 mRy.  
 [30] B. Johansson, L. Fast, P. Söderlind, and O. Eriksson, *Physica (Amsterdam)* **190B**, 12 (1993).